A_1 and A_2 Production in the Reaction $\pi^-+p \to \pi^-+\pi^-+\pi^++p$ at 7.0 BeV/c*

NEAL M. CASON†
University of Wisconsin, Madison, Wisconsin
(Received 7 March 1966)

Two-hundred thirteen events of the type $\pi^-+p \to \pi^-+\pi^-+\pi^++p$ occurring in the Shutt 20-in. hydrogen bubble chamber at an incident-beam momentum of 7.0 BeV/c have been analyzed. The event separation has been performed utilizing kinematic fitting and ionization criteria. The contamination of the sample due to other final states is less than 10%. The cross section for this reaction has been measured to be 1.7±0.2 mb. The partial cross sections for the production of resonant final states have been measured with the results: $\sigma(\pi^-+p \to \pi^-+\pi^-+N^{*++})=0.55\pm0.11$ mb; $\sigma(\pi^-+p \to \pi^-+\rho^0+p)=0.38\pm0.10$ mb; and $\sigma(\pi^-+p \to N^{*0}+\rho^0)=0.035\pm0.013$ mb. The N^{*++} isobar mass and width were found to be 1216±14 MeV and 114±30 MeV, respectively. The ρ^0 parameters are $M^*=773\pm12$ MeV and $\Gamma=57_{-15}^{+25}$ MeV. ρ^0 production is peripheral and is dominated by final states with low $\pi^-\rho^0$ effective mass; limited statistics prevent us from resolving this enhancement into the A_1 and the A_2. Angular distributions in the $\pi^-\rho^0$ and the ρ^0 rest frames are presented as a function of the $\pi^-\rho^0$ mass. Conclusions drawn about the spin-parity of the A_1 and the A_2 from these distributions are highly model-dependent The model used indicates that the most likely spin-parity assignments for the A_2 are, in order of likelihood, 2^-, 1^-, or 1^+. If the A_1 is a resonance rather than a kinematic reflection, its most likely spin-parity assignments are 1^+ or 2^-.

INTRODUCTION

THE 20-in. hydrogen bubble chamber located at Brookhaven National Laboratory has been exposed to a beam of 7.0 BeV/c negative pions. We present here a report on the reaction

$$\pi^-+p \to \pi^-+\pi^-+\pi^++p.$$

This reaction (as well as that involving an incident π^+) has been studied at several other laboratories[1–3] where it has been shown that the $\pi^\mp\rho^0p$ final state is dominated by enhancements in the $\pi^\mp\rho^0$ mass spectrum at 1072 MeV (A_1) and at 1324 MeV (A_2).

Several explanations of the A_1 as a kinematic reflection of particular production mechanisms have been put forward. The suggestions of Deck,[4] modified by O'Halloran and Maor,[5] have been shown to be consistent with the data at 3.65 BeV/c.[6] The current evidence[7] suggests that the A_1 has $J^p=1^+$ (π-ρ s wave) or 2^- if it is a resonance rather than a kinematic reflection.[8]

The A_2 is more likely a resonance than a kinematic reflection. An enhancement in the $K\bar{K}$ system[2] has been observed at about the same mass as the A_2.[8] The lowest spin-parity assignment which is consistent with both a $\rho\pi$ and a $K\bar{K}$ decay is 2^+. If on the other hand this $K\bar{K}$ enhancement is not associated with the A_2,[9] then current evidence[7] is most consistent with spin-parity assignments of 2^+, 2^-, or 1^+.

In π^-p collisions at 7 BeV/c, we have two advantages in studying A-meson production. First, since there is only one π^+ in the final state, the separation of the competing N^{*++} isobar production is fairly straightforward. Secondly, the high incident-beam momentum yields a sample of A's with much less background than at lower momentum. We are therefore able to study angular correlations with a reasonably clean sample of events.

EXPERIMENTAL PROCEDURE

An aluminum target in the shape of a pencil was wiped across the bottom of the internal beam of the A.G.S. The effective target size normal to the internal beam was about 1 cm×0.1 cm. The secondary beam then emerged from the F-10 straight section at 4.8° to the internal beam.

The beam was collimated by a 1-in.-square slit located just before a bending magnet. This magnet bent the beam by 4° and was set to select particles of momentum 7.0 BeV/c. The beam was then sent through a 4-in.-square channel in the wall. The finite aperture of this momentum collimator was expected to result in a spread of the beam momentum of about ±2%. The beam then entered the bubble chamber. No other elements were present in the beam.

About 15 000 pictures were taken. The average num-

* Work supported in part by the U. S. Atomic Energy Commission.
† Present address: Department of Physics, University of Notre Dame, Notre Dame, Indiana.
[1] G. Goldhaber, J. L. Brown, S. Goldhaber, J. A. Kadyk, B. C. Shen, and G. H. Trilling, Phys. Rev. Letters **12**, 336 (1964).
[2] S. U. Chung, O. I. Dahl, L. M. Hardy, R. I. Hess, G. R. Kalbfleisch, J. Kirz, D. H. Miller, and G. A. Smith, Phys. Rev. Letters **12**, 621 (1964).
[3] Aachen-Berlin-CERN Collaboration, Phys. Letters **12**, 356 (1964).
[4] R. T. Deck, Phys. Rev. Letters **13**, 169 (1964).
[5] U. Maor and T. A. O'Halloran, Jr., Phys. Letters **15**, 281 (1965).
[6] B. C. Shen, G. Goldhaber, S. Goldhaber, and J. A. Kadyk, Phys. Rev. Letters **15**, 731 (1965).
[7] R. L. Lander, M. Abolins, D. D. Carmony, T. Hendricks, N. Xuong, and P. M. Yager, Phys. Rev. Letters **13**, 346 (1964).
[8] No alternative decay modes of the A_1 have been observed and confirmed, although some evidence for $\eta\pi$ decay modes for both the A_1 and the A_2 has been presented. See Aachen-Berlin-Birmingham-Bonn-Hamburg-London(I.C.)-Munchen Collaboration, Phys. Letters **10**, 226 (1964). The spin parity for a resonance which decays into both $\rho\pi$ and $\eta\pi$ is 1^-, 2^+, 3^-, ⋯.
[9] Data from an experiment at 8 GeV/c seems to indicate no $K\bar{K}$ or $\eta\pi$ decay modes for the A_2. See D. R. O. Morrison, Bull. Am. Phys. Soc. **10**, 485 (1965).

ber of tracks per picture was about 20, but the number of tracks per picture varied over a large range. Fluctuations in the chamber operating conditions and camera operation occasionally produced large variations in picture quality. Therefore the film was edited by looking at every frame and classifying it as unusable (8.8% of the pictures), acceptable for analysis but not for cross section determination (8.7%), or acceptable for all purposes (82.5%).

The interactions used in this experiment were required to occur in a restricted fiducial volume defined by placing a template on the projected image of view 2. The interaction point was required to fall within the boundaries of the template. We were left with a fiducial volume of approximately 13.0 cm in the beam direction and 8.0 cm transverse to the beam. The restriction to 13.0 cm in the beam direction utilizes only about $\frac{1}{3}$ of the length of the chamber. This was necessary in order to assure a reasonable momentum determination of high-momentum secondaries.

In two independent scans, 1216 four-prong events were found which occurred in the fiducial volume. This sample of events had no obvious strange-particle decays; also, for all tracks which had secondary interactions, it was required that the interacting track have a projected length of more than 10 cm. These events comprise the sample used in this experiment. An over-all scanning efficiency of 99.8% was determined for four prongs in that portion of the film used for cross-section purposes by comparing the results of the two scans.

The events were measured in three views on digitized measuring machines. Each track was then reconstructed in the three separate view-pairs by SPACE.[10] This program fits an ellipse through the measured points and requires the tracks to meet at a common vertex.

All tracks were required to be measured to their end, to have a low point-setting error, and to be strictly consistent in momentum and angles from one view-pair to another.

To experimentally determine the beam momentum, 60% of the measured events were run through the kinematic fitting routine GUTS,[11] trying the hypothesis $\pi^-+p\rightarrow\pi^-+\pi^-+\pi^++p$ without specifying the incident beam momentum. One-hundred thirty-five events gave a three-constraint $\chi^2<11.0$, and were consistent with the reaction with respect to ionization. The average fitted beam momentum for these 135 events is 6.97 $\pm$0.03 BeV/c. The momentum spread including measuring resolution is 4.2% (0.29 BeV/c).

After spatial reconstruction, each event was tested in GUTS for kinematical consistency with the following reactions:

$$\pi^-+p\rightarrow\pi^-+\pi^-+\pi^++p, \quad (1)$$

$$\pi^-+p\rightarrow\pi^-+\pi^-+\pi^++p+\pi^0, \quad (2)$$

$$\pi^-+p\rightarrow\pi^-+\pi^-+\pi^++\pi^++n. \quad (3)$$

Of the 1216 events processed, 217 fit reaction (1) with $\chi^2<15.0$. Because of the large spread in beam momentum, reactions (2) and (3) could not be analyzed in this experiment.

All of the 1216 events were examined by experienced personnel to determine the relative ionization of each of the secondaries. The output for each of the 217 events fitting reaction (1) was compared with this ionization data. Only 3 events were inconsistent with the data. One other event was eliminated because an electron pair pointed to the vertex of the event. We were thus left with a sample of 213 events which are consistent with reaction (1).

Besides checking ionization, the following checks have been made to assure that our sample is free from background:

1. The unconstrained missing mass-squared distribution is symmetric with no peak in the π^0 mass region. The distribution is quite sharp with a full width at half-maximum of 0.010 BeV^2.

2. The missing energy distribution is symmetric about zero.

3. We have compared the one-constraint χ^2 distribution for events which fit only the one-constraint hypothesis with the distribution for those events which are ambiguous between a one-constraint and a four-constraint hypothesis. In the former case a typical one-constraint distribution is found, whereas in the latter case an essentially flat distribution is found.

4. For these same two classes of events the π^0 momentum spectra are compared. For unambiguous events, the spectrum is similar to the π^+ or π^- spectra. When the ambiguous events are added to the unambiguous events, the π^0 spectrum is very different, having a very large peak in the range 0–100 MeV.[12]

Our conclusion is that we have no evidence that our sample contains any background from events with five or more particles in the final state. An upper limit of 10% can be placed on the over-all contamination.

DATA ANALYSIS

Cross-Section Determination

We have determined cross sections for this experiment by counting the total number of interactions occurring within the restricted fiducial volume and then normalizing to the total cross section of 28.4$\pm$0.6 mb

[10] This program was written by A. Erwin and D. Lyon at the University of Wisconsin.

[11] J. P. Berge, F. T. Solmitz, and H. D. Taft, UCRL 9097 (1960), GUTS has been incorporated into a general program to analyze 4-prong events by P. Satterblom at the University of Wisconsin.

[12] In addition to these checks, the possibilities of contamination by Dalitz pair events and by strange-particle events were examined and found to be negligible.

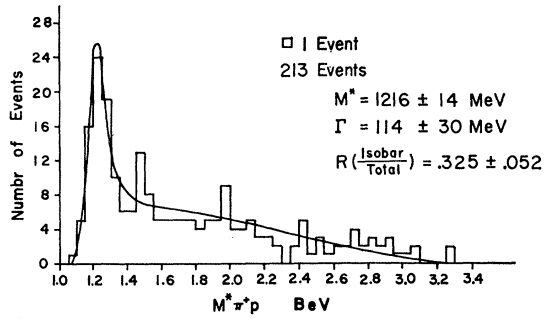

FIG. 1. Distribution of the π^+p effective mass for the 213 events which fit the reaction $\pi^-p \to \pi^-+\pi^-+\pi^++p$. The smooth curve is a maximum likelihood fit to the data (see text), and is normalized to all events.

measured by von Dardel *et al.*[13] The result is thus independent of the μ^- contamination. The K^- and $\bar{p}$ contaminations are negligible.

For cross-section purposes 82.5% of the film was used. Sixty-one percent of this film was scanned for all beam-track interactions with charged-particle secondaries. After correcting for zero prongs and low-momentum-transfer elastic events,[14] we find

$$\sigma(\pi^-+p \to \pi^-+\pi^-+\pi^++p)=1.7\pm0.2 \text{ mb}.$$

The error includes both the statistical error and the uncertainty in normalization.

In the entire experiment we found 213 events of this type. Thus all partial cross sections in this sample will be based on 8 μb/event.

Isobar Production

Figure 1 shows the (π^+p) mass distribution for the 213 events. It is obvious that the production of the 3-3 isobar is important in these data. The smooth curve shown is of the form

$$F(x,M^*,\Gamma,f)=((1-f)\phi_4(x)/N_1)+(f\phi_4(x)B(x)/N_2),$$

where x is the (π^+p) mass; M^* is the isobar mass; $\phi_4(x)$ is phase space for two out of four particles; N_1 and N_2 are appropriate normalization constants; f is the fraction of events where the isobar is produced; and $B(x)$ is a Breit-Wigner function of the form

$$B(x)=(\Gamma/2)/[(M^*-x)^2+(\Gamma/2)^2].$$

In other words, the function is the incoherent sum of a phase-space term and a term with a Breit-Wigner shape modified by phase space. We have computed the likelihood function,

$$L(M^*,\Gamma,f)=[\prod_{i=1}^{213} F(x_i,M^*,\Gamma,f)]/N(M^*,\Gamma,f),$$

and have varied the parameters to maximize this function. (N is the appropriate normalization factor.) The smooth curve shows the results of this fit. As one can see in Fig. 1, the good fit to the data indicates that the form of F is sufficient to explain the data. The fitted parameters are

$$M^*=1216\pm14 \text{ MeV},$$
$$\Gamma=114\pm30 \text{ MeV},$$
$$f=0.325\pm0.052.$$

The errors are chosen at the point where the likelihood decreases by a factor of $e^{-1/2}$. The isobar parameters are in good agreement with other experiments. Since 32.5% of the events are isobar events, we find that

$$\sigma(\pi^-+p \to \pi^-+\pi^-+N^{*++})=0.55\pm0.11 \text{ mb}.$$

ρ Production

We now wish to study the final state $\pi^-\rho^0p$. Since there is only one π^+ in our final state, isobar production and ρ production are independent except for possible interference effects. Furthermore, a scattergram of $M^*(\pi^+p)$ versus $M^*(\pi^+\pi^-)$ indicates that the ρ^0-N^{*++} overlap region is consistent with simple superposition of the two resonant bands, and thus there appears to be very little interference between the two resonances.

In order to study the ρ^0 production process more clearly, the analysis which follows will be done after removing events in the region

$$1100<M^*(\pi^+p)<1330 \text{ MeV}.$$

There are 73 events in this region of which about 20 events are not isobar events. Thus we have separated 140 "nonisobar" events from the total sample. The contamination of this sample due to the tail of the isobar curve is about 10%.

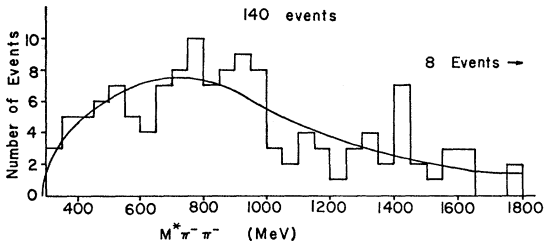

FIG. 2. Distribution of the $\pi^-\pi^-$ effective mass for the 140 nonisobar events. The smooth curve is phase space, based on the 3-pion effective-mass distribution, and is normalized to all the events.

[13] G. von Dardel, R. Mermod, P. A. Piroe, M. Vivargent, G. Weber, and K. Winter, Phys. Rev. Letters **7**, 127 (1961). We have increased the uncertainty quoted by the authors to take into account their stated uncertainty in normalization.

[14] The cross section for zero prongs is 1.5±0.5 mb. [R. A. Aripov, V. G. Grishin, L. V. Silvestrov, and V. N. Strelstsov, Zh. Eksperim. i Teor. Fiz. **43**, 394 (1962), [English transl.: Soviet Phys.—JETP **16**, 283 (1963)]. The correction for scanning loss due to low-momentum-transfer elastic-scattering events was taken from another experiment [S. Brandt, V. T. Cocconi, D. R. O. Morrison, A. Wroblewski, P. Fleury, G. Kagas, F. Muller, and C. Pelletier, Phys. Rev. Letters **10**, 413 (1963)]. This correction was 1.0±0.2 mb.

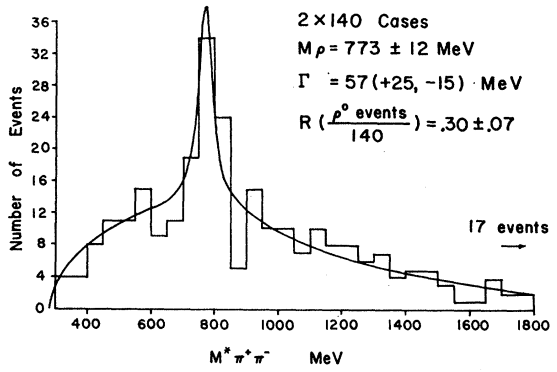

FIG. 3. Distribution of the $\pi^+\pi^-$ effective mass for the 140 nonisobar events. Each event is plotted twice. The smooth curve is a maximum-likelihood fit to the data (see text), and is normalized to all the events.

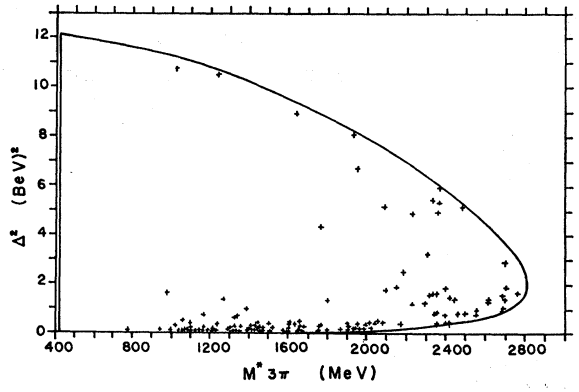

FIG. 4. Scattergram of the square of the four-momentum transfer from the initial proton to the final proton versus the $\pi^-\pi^-\pi^+$ effective mass for the 140 nonisobar events. The boundary represents the kinematical limit.

Figure 2 is the $(\pi^-\pi^-)$ mass spectrum for these events. The normal phase-space curve (not shown) for two particles out of four gives a poor fit to these data. This is due to the fact that, as we will see, the three-pion effective-mass spectrum is heavily weighted toward low three-pion effective masses, thus weighting our two-pion spectrum toward low mass values. The smooth curve shown in Fig. 2 is a modified phase-space curve which has the experimental three-pion mass distribution folded into it. The curve is of the form

$$f(x)=\sum_{i=1}^{140}\phi_3(x,E_i)\Big/\int_{2m_\pi}^{E_i-m_\pi}\phi_3(x,E_i)dx,$$

where x is the $(\pi^-\pi^-)$ mass, E_i is the $(\pi^-\pi^-\pi^+)$ mass, and $\phi_3(x,E_i)$ is phase space for two particles out of three. The good fit of the data to this curve, which is normalized to all the events, shows that the $(\pi^-\pi^-)$ mass distribution can be explained completely in terms of the three-pion distribution.

Figure 3 is the $(\pi^+\pi^-)$ mass distribution for the same events. There are two entries for every event. The smooth curve is a maximum-likelihood fit to the data of the same form used for the (π^+p) distribution. (However, the modified phase-space curve defined for the $\pi^-\pi^-$ distribution was used instead of four-body phase space since the $\pi^+\pi^-$ spectrum will also be distorted by the low three-pion effective-mass enhancements.) The fitted parameters are

$$M^*=773\pm12\text{ MeV},$$
$$\Gamma=57_{-15}^{+25}\text{ MeV},$$
$$\text{Number of }\rho^0\text{ events}/140=0.30\pm0.07.$$

Our measured values for the mass and width of the ρ^0 are about two standard deviations[15] from the accepted values ($M^*=754$ MeV, $\Gamma=110$ MeV), and thus are just compatible with these values. It is possible that final-state interactions prevent experimenters from observing the true mass and width of the ρ^0. If such is the case, it would lead to discrepancies between the values obtained at different energies and in different reactions. Our data come from very low momentum transfers to the proton and hence we may have the ρ^0 isolated from the final-state proton.[16]

The value of the cross section for ρ^0 production, after taking into account the events lost due to the isobar-subtraction technique is

$$\sigma(\pi^-+p\rightarrow\pi^-+p+\rho^0)=0.38\pm0.10\text{ mb}.$$

A scattergram of $M^*(3\pi)$ versus Δ^2 (the square of the 4-momentum transfer from the initial proton to the final proton) is shown in Fig. 4, along with the kinematic

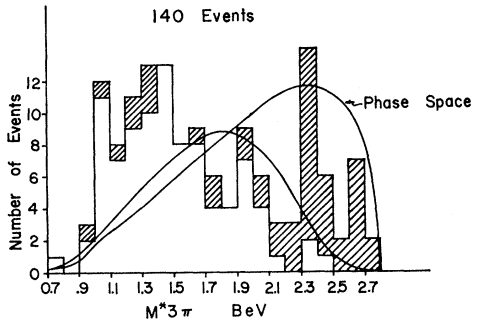

FIG. 5. Distribution of the $\pi^-\pi^-\pi^+$ effective mass for the 140 nonisobar events. The cross-hatched events have $\Delta^2>0.5$ BeV^2. The phase-space curve is 70% 4-body phase space and 30% 3-body $(\pi^-\rho^0 p)$ phase space. It is normalized to all events. The second curve shown is phase space folded in with the observed 4-momentum-transfer distribution, and is normalized to the low-momentum-transfer events.

[15] The likelihood function for M^* is Gaussian. The likelihood function for Γ is not Gaussian, but its likelihood at $\Gamma=110$ MeV is 4% of its likelihood at 57 MeV. Hence, it is equivalent to being two standard deviations from the accepted value.

[16] A recent experiment [Y. Y. Lee, Ph.D. thesis, University of Michigan, Ann Arbor, Michigan, 1964 (unpublished)] studying the reaction $\pi^-+p\rightarrow\rho^0+n$ has presented evidence that the mass and width of the ρ^0 are functions of momentum transfer to the nucleon. This experiment indicates a higher mass and narrower width for lower momentum transfers to the nucleon.

limits for our energy, for the 140 nonisobar events. The highly peripheral nature of the interactions is clearly seen from the preponderance of low momentum-transfer events. The momentum-transfer distribution is fit quite well by the function of the form $A\exp(-7.3\Delta^2)$ which is the function which characterizes π^--proton elastic scattering at this energy.[17]

Figure 5 gives the projection of this plot on the $M^*(3\pi)$ axis. The cross-hatched events in this plot are the events with $\Delta^2>0.5$ (BeV/c).[2] The curve labeled phase space consists of 70% 4-body phase space and 30% 3-body ($\pi\rho p$) phase space. This curve is normalized to the total number of events. It is quite clear that the three-pion mass distribution does not follow a phase-space distribution. The tendency for low values of 3-pion mass is clear.

In order to see if the phase-space contraction caused by the low-momentum-transfer nature of the reaction can explain this 3-pion effective-mass spectrum, we have shown in Fig. 5 a second curve which is phase space multiplied by

$$\int_{-1}^{1}\exp(-7.3\Delta^2)d(\cos\theta)\,,\quad\text{where}\quad\Delta^2=\Delta^2[\cos\theta,M^*(3\pi)]\,.$$

This amounts to folding in the observed Δ^2 distribution with a phase-space distribution. This second curve is normalized to the low-momentum-transfer events and illustrates that the very narrow Δ^2 distribution for these events does *not* account for the large discrepancy between the phase space and the data.

We now show that ρ^0 events contribute significantly

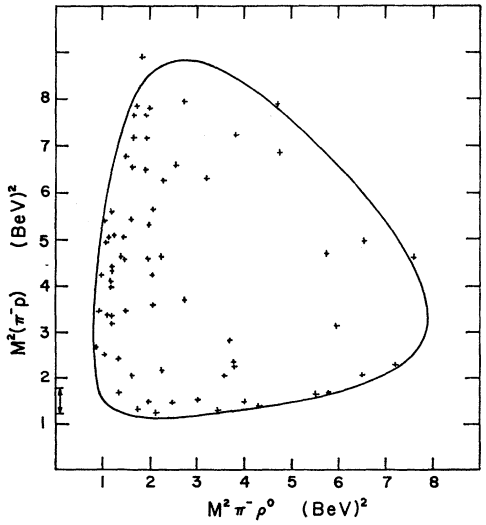

FIG. 6. Dalitz plot for the 68 events in the ρ^0 region. The boundary for a ρ^0 mass of 775 MeV is shown. The position of the 3-3 isobar is shown on the $M^2(\pi^-p)$ axis.

[17] K. J. Foley, S. J. Lindenbaum, W. A. Love, S. Ozaki, J. J. Russell, and L. C. L. Yuan, Phys. Rev. Letters **10**, 376 (1963).

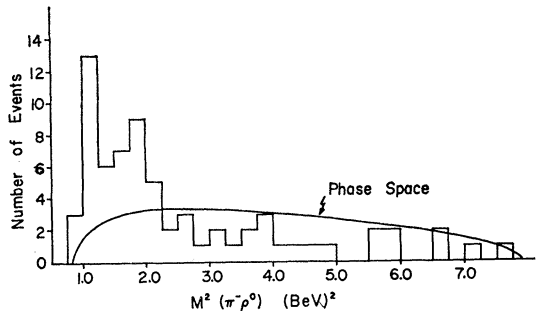

FIG. 7. Distribution of the square of the $\pi^-\rho^0$ effective mass for the 68 ρ^0 events. The smooth curve is phase space.

to the enhancement. ρ^0 events, are selected by requiring

$$700\leq M^*(\pi^+\pi^-)\leq 850\text{ MeV}.$$

Of the 140 nonisobar events, 68 satisfy this requirement. We estimate that 62% of these events are ρ^0 events, the remainder being background. These events are entered on a Dalitz plot in Fig. 6 where $M^2(\pi^-p)$ is plotted versus $M^2(\pi^-\rho^0)$. The boundary for a ρ^0 of mass 775 MeV is shown. In those cases with 2 values of $M^*(\pi^+\pi^-)$ in the ρ^0 region, we have chosen as the ρ^0 the $(\pi^+\pi^-)$ pair nearest 775 MeV.

The Dalitz plot shows two features of interest. First it is clear that there again is an enhancement in the low $(\pi^-\rho^0)$ effective-mass region. Not so obvious but statistically significant is a band of events with $M^{*2}(\pi^-p)$ in the N^{*0} region. If we project on the $M^{*2}(\pi^-p)$ axis and count the number of events above the phase-space estimate in the isobar region, we find

$$\sigma(\pi^-+p\rightarrow N^{*0}+\rho^0)=0.035\pm0.013\text{ mb}.$$

The events in this band are subtracted in the following analysis.

In Fig. 7 is shown the projection of the Dalitz plot on the $M^2(\pi^-\rho^0)$ axis. The smooth curve is phase-space normalized to all events. The clumping at low $\pi^-\rho^0$ effective mass is again clear. This is in the region where the A_1 and A_2 have been observed. The small number of events in our experiment does not allow us to resolve two peaks, but in the analysis to follow, we shall assume that there are two different effects, the A_1 between 1.0 and 1.2 BeV and the A_2 between 1.2 and 1.4 BeV. From Fig. 7 we estimate that the low-mass region of the $\pi^-\rho^0$ spectrum is 75% pure A_1 or A_2 in their respective mass regions.

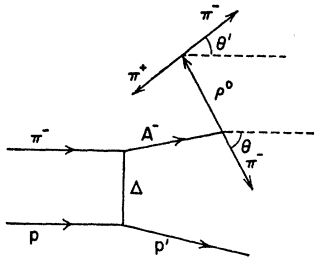

FIG. 8. Diagram illustrating the definition of the angles θ and θ'.

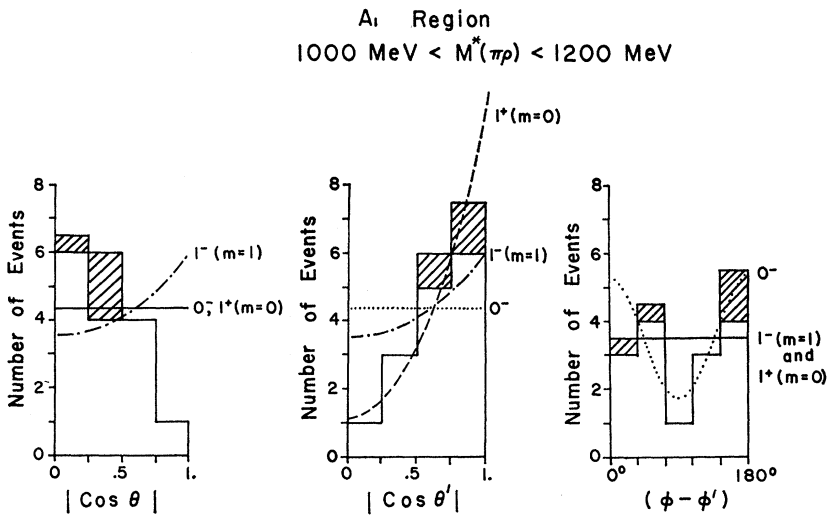

FIG. 9. Internal angular distributions for the 17.5 events in the A_1 region. The cross-hatched events are weighted events from the ρ-isobar overlap region (see text). The angles are defined in the text.

Prior to studying angular distributions in the A_1 and A_2 regions, we will attempt to remove biases which may have been introduced by our isobar-subtraction technique. We now put back into our sample those events which are in the ρ-isobar overlap regions with a statistical weight which is the ratio of the number of events expected in the region[18] to the number observed. (This weighting factor is 0.5 for both the N^{*++} and the N^{*0}.) These events are shown as cross-hatched events in all the angular distributions. It will be noted that these events do not significantly change the character of any distribution.

Figure 8 shows the coordinate systems used in defining θ and θ'. θ is the angle between the recoil π^- from A decay and the beam π^- in the A rest frame. The beam direction is then transformed into the ρ^0 rest frame; θ' is defined as the angle between this direction and the π^- from the ρ^0 decay in the ρ^0 rest frame. ϕ and ϕ' are the corresponding azimuths.[19]

Figures 9 and 10 show the distributions in θ, θ', and in ϕ-ϕ' for the A_1 and the A_2 regions, respectively. The poor statistics does not warrant a highly sophisticated model. We, therefore, make the following simple assumptions:

1. A-meson production is dominated by the exchange of a single particle having either spin 0 or spin 1.[20]

2. If the spin-1 exchange dominates, the exchanged particle is polarized predominately along or transverse to its direction. In this way we can assume that the initial state is either an $m=1$ or an $m=0$ state.

[18] The number of events expected in the region is determined from the area under the (π^+p) or (π^-p) phase-space curve in the isobar region when normalized to the total number of events, assuming no isobar is present. This is done for ρ^0 events, and assumes that there is no interference between isobar production and ρ^0 production.

[19] ϕ-ϕ' is independent of an arbitrary azimuthal rotation and therefore no production-plane normal direction is used.

[20] Single-pion exchange is forbidden by the conservation of G parity, so the exchanged particle can be an η^0 or a ρ^0.

TABLE I. Predicted angular distributions for the model described in the text. J is the total angular momentum of the π-ρ system. The m values indicated refer to the state of polarization of the exchanged particle where the axis of the quantization is the beam-track direction.

J^P	$f(\theta,\phi,\theta',\phi')$
0^-	$(3/16\pi^2)[\sin^2\theta\sin^2\theta'\cos^2(\phi-\phi')+\cos^2\theta\cos^2\theta'$ $+2\cos\theta\sin\theta\cos\theta'\sin\theta'\cos(\phi-\phi')]$
$1^-(m=1)$	$(9/64\pi^2)[\cos^2\theta\sin^2\theta'+\sin^2\theta\cos^2\theta'$ $-2\cos\theta\sin\theta\cos\theta'\sin\theta'\cos(\phi-\phi')]$
$1^-(m=0)$	$(9/32\pi^2)\sin^2\theta\sin^2\theta'\cos^2(\phi-\phi')$
$1^+(m=0)$	$(3/16\pi^2)\cos^2\theta'$
$1^+(m=1)$	$(3/32\pi^2)\sin^2\theta'$
$2^-(m=0)$	$(3/8\pi^2)[\cos^2\theta\cos^2\theta'+\frac{1}{4}\sin^2\theta\sin^2\theta'\cos^2(\phi-\phi')$ $-\cos\theta\cos\theta'\sin\theta\sin\theta'\cos(\phi-\phi')]$
$2^-(m=1)$	$(9/64\pi^2)[\cos^2\theta\sin^2\theta'+\sin^2\theta\cos^2\theta'$ $+2\sin\theta\cos\theta\sin\theta'\cos\theta'\cos(\phi-\phi')]$
$2^+(m=1)$	$(15/64\pi^2)[\frac{1}{2}(5\cos^4\theta-4\cos^2\theta+1)$ $-\frac{1}{2}\cos^2\theta'(7\cos^4\theta-6\cos^2\theta+1)$ $-\sin\theta\cos^3\theta\sin2\theta'\cos(\phi-\phi')$ $-\frac{1}{2}(1-\cos^2\theta')(3\cos^4\theta-4\cos^2\theta+1)\cos^2(\phi-\phi')]$
$2^+(m=0)$	$(45/32\pi^2)(\cos^2\theta-\cos^4\theta)\sin^2\theta'\sin^2(\phi-\phi')$

3. The 25% background is noninterfering and isotropic.

4. The angular distributions are not distorted too greatly by absorption effects.

If these four assumptions are approximately correct, then for each value of the spin parity of the A mesons, and for each exchange process, we can compute the distributions in θ, θ' and ϕ-ϕ'. The predicted distributions are given in Table I, and some of the predicted curves are shown in Figs. 9 and 10.

The likelihood of our observed distributions was then computed for each of the predicted functions $f(\theta,\theta',\phi\text{-}\phi')$. The likelihoods are given by

$$L=\prod_{i=1}^{n} f(\theta_i,\theta_i',\phi_i-\phi_i'),$$

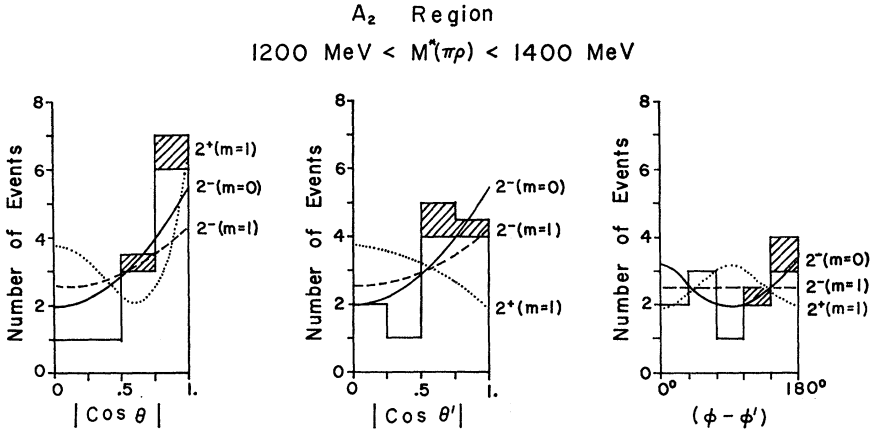

FIG. 10. Internal angular distributions for the 12.5 events in the A_2 region. The cross-hatched events are weighted events in the ρ-isobar overlap region (see text). The angles are defined in the text.

where n is the number of events in the $\pi^-\rho^0$ mass region under consideration. Table II gives these likelihoods relative to the most likely function for every case.

The significance of these likelihoods might be clarified by the following observations. First, the likelihood includes correlations between the distributions in θ, θ', and ϕ-ϕ'. Secondly, although the distribution with the greatest likelihood is most consistent with the data, no distribution can be ruled out in the absence of a goodness-of-fit criterion.[21] Finally, although the likelihood ratios give betting odds for choosing which function is correct, the ratios should be considered at best as order of magnitude estimates. This is due to the fact that the significance of the ratios is a function of several variables, such as the number of events and the form of the functions being fitted, and a systematic study of the confidence levels was deemed inappropriate for such a small sample of events.

TABLE II. Relative likelihoods in the A_1 and A_2 regions for various assumptions of the A spin parity and of the polarization of the exchanged particle. Likelihoods relative to the most likely case are shown. The forbiddeness of the process is indicated for spin-1 and spin-0 exchange.

J^P	Relative likelihood A_1	Relative likelihood A_2	Allowed for Spin-0 exchange	Allowed for Spin-1 exchange
0^-	1/245	1/4260	Yes	Yes
$1^-(m=1)$	1/113	1/17.5	No	Yes
$1^-(m=0)$	1/736	$1/10^5$	Yes	No
$1^+(m=0)$	1/1	1/21.6	Yes	Yes
$1^+(m=1)$	$1/10^4$	1/3640	No	Yes
$2^-(m=0)$	$1/10^5$	1/1	Yes	Yes
$2^-(m=1)$	1/7.8	1/75.5	No	Yes
$2^+(m=1)$	$1/10^5$	1/83	No	Yes
$2^+(m=0)$	$1/10^8$	$1/10^5$	Yes	No

[21] Since this sample of events is so small, normal statistical tests, such as standard χ^2 tests, fail. Goodness of fit must be determined in another manner. Although a rigorous method can be devised (e.g. using a Monte Carlo technique), we have not carried out such a calculation because the data seem insufficient to warrant such treatment.

The results are that the A_1 is most likely 1^+ if the exchanged particle has spin 0 or has $m=0$, and is most likely 1^+ or 2^- if it has $m=1$. This is quite consistent with other results using only symmetry arguments.[7] For the A_2, the most likely state is 2^- for spin 0 (or $m=0$) exchange, and is in order of likeliness, 2^-, 1^-, or 1^+ otherwise. This result is consistent with the recent results of Barnes *et al.*[22] who again use only symmetry arguments. 2^+ which is required if the $K\bar{K}$ bump at 1310 MeV observed by Chung *et al.*[2] is an alternate decay mode of the A_2, is unlikely relative to 2^- by odds of 83:1.

CONCLUSIONS

1. We have shown that, in spite of both the high-beam momentum and the rather broad-beam momentum width, the event sample used in this experiment is quite free from background.

2. A summary of the cross sections measured is given in Table III. Also shown there are the resonant masses and widths for the resonant final states.

3. The reaction $\pi^-+p \rightarrow \pi^-+\rho^\circ+p$ is dominated by low momentum transfer from the initial proton to the final proton and by the production of a final state with $1.0<M^*(\pi\rho)<1.4$ BeV. Our data clearly show that this final state is neither a kinematic reflection of the low-

TABLE III. Summary of the cross sections and resonance parameters measured in this experiment.

Final state	Cross section (mb)	Resonant mass (MeV)	Resonant width (MeV)
$\pi^-\pi^-\pi^+p$	1.7 ±0.2		
$\pi^-\pi^-N^{*++}$	0.55 ±0.11	1216±14	114±30
$\pi^-\rho^0p$	0.38 ±0.10	773±12	57_{-15}^{+25}
ρ^0N^{*0}	0.035±0.013		

[22] V. E. Barnes, W. B. Fowler, K. W. Lai, S. Orenstein, D. Radojicic, M. S. Webster, A. H. Bachman, P. Baumel, and R. M. Lea, Phys. Rev. Letters 16, 41 (1966).

momentum-transfer distribution or of 3-3 isobar production.[23]

4. If the A_1 is a resonance, then our most likely assignments for its spin parity are $J^P=1^+$ (s wave) or 2^-.

5. The most likely spin parity assignments for the A_2 are $J^P=2^-$, 1^-, or 1^+ in our highly model-dependent calculation.

[23] Barnes *et al.* (Ref. 22) state that they have no peak in the A_1 region when the isobar events are removed. Their data do show an excess of events in the A_1 region after the subtraction, but this excess is in the form of a broad shoulder rather than a peak. The number of events in our experiment is too small to tell the difference between a peak and a shoulder, but we can tell that there is an excess of events in the A_1 region after subtracting isobar events.

ACKNOWLEDGMENTS

I would like to express my sincere appreciation to Dr. M. L. Good for his guidance and support during this experiment. The support of Dr. W. D. Walker is also gratefully acknowledged. Many enlightening discussions with Dr. C. Goebel guided some of the theoretical aspects of this work. Finally, I would like to thank Brookhaven National Laboratory and the 20-in. bubble chamber operating crew for their help in the experiment.

PHYSICAL REVIEW VOLUME 148, NUMBER 4 26 AUGUST 1966

Polarization Parameter in p-p Scattering from 328 to 736 MeV*

F. BETZ,† J. ARENS, O. CHAMBERLAIN, H. DOST,‡ P. GRANNIS, M. HANSROUL, L. HOLLOWAY, C. SCHULTZ,§ AND G. SHAPIRO

Lawrence Radiation Laboratory, University of California, Berkeley, California

(Received 17 March 1966)

The polarization parameter in elastic proton-proton scattering has been measured using an unpolarized proton beam and a polarized proton target. Measurements were taken at laboratory kinetic energies of 328, 614, 679, and 736 MeV in the angular regions from 33 to 110 degrees center-of-mass. The results indicate that the maximum polarization at a given energy increases in the region from 328 to 679 MeV. At 328 MeV the results are in good agreement with those of a previous experiment at 315 MeV performed by the double-scattering technique.

I. INTRODUCTION

ALTHOUGH the phenomenological description of the proton-proton interaction has been in a fairly satisfactory state for several years up to kinetic energy 300 MeV,[1] extension of this knowledge to higher energies has been slow, owing in part to the relative scarceness of experimental data, and in part to the rapidly increasing number of parameters required.[2] From the work done up to 300 MeV, as well as that on the pion-nucleon interaction,[3] it appears that a promising road to a satisfactory description of the nucleon-nucleon interaction lies in an energy-dependent phase-shift analysis. For this reason we have measured the polarization in elastic p-p scattering at several energies between 300 and 740 MeV. The availability of a polarized proton target enabled us to take data at a greatly increased rate compared to the formerly used double-scattering technique, as well as at many angles simultaneously, and also enabled us to avoid some of the sources of systematic errors common in double-scattering experiments, such as spurious asymmetries due to counter misalignment and uncertainties in the angular and energy dependence of the analyzing power.

Because of the spin-state multiplicity of the nucleon-nucleon system, a large number of independent experiments must be performed at each energy if the phenomenological analysis is to have any hope of success. These include, in addition to cross-section and polarization measurements, "triple-scattering" and spin-correlation experiments as well as investigations of the inelastic processes. Some of these have been performed at various laboratories, and we have recently completed a measurement of C_{NN} as a function of angle at 680 MeV, using a polarized beam and polarized target.[4] Still, a number of other types of experiments will be needed before a phase-shift analysis can be completed.

The formal description of nucleon-nucleon scattering has been carried out by a large number of authors in

* Work done under the auspices of the U. S. Atomic Energy Commission.

† Present address: Space Sciences Laboratory, University of California, Berkeley, California.

‡ Present address: Center of Naval Analysis, Arlington, Virginia.

§ Present address: Columbia University, New York, New York.

[1] M. H. MacGregor, M. J. Moravcsik, and H. P. Strapp, Ann. Rev. Nucl. Sci. **10**, 291 (1960).

[2] See, however, R. Ya. Zue'karnerv and I. N. Silin, Phys. Letters **3**, 265 (1963); N. Hoshizaki and S. Machida, Research Institute of Fundamental Physics Report No. RIFP-30, Kyoto University, 1963 (unpublished).

[3] L. D. Roper and R. M. Wright, Phys. Rev. **138**, B921 (1965).

[4] H. E. Dost, J. F. Arens, F. W. Betz, O. Chamberlain, M. J. Hansroul, L. E. Holloway, C. H. Schultz, and G. Shapiro, Bull. Am. Phys. Soc. **9**, 724 (1964).